JOURNAL OF PROPULSION AND POWER
Vol. 25, No. 6, November–December 2009

# Quasi-One-Dimensional Model of Hydrogen-Fueled Scramjet Combustors

Cristian Birzer* and Con J. Doolan†
*The University of Adelaide, Adelaide, South Australia 5005, Australia*

DOI: 10.2514/1.43716

**A computationally efficient, quasi-one-dimensional, supersonic combustion ramjet (scramjet) propulsion model has been produced for use in hypersonic system design studies. The model solves a series of ordinary differential equations using a fourth-order Runge–Kutta method to describe the gas dynamics within the scramjet duct. Additional models for skin friction and wall heat transfer are also included. The equations are derived assuming an open thermodynamic system with equilibrium or simplified-chemistry combustion models. The combustion is also assumed to be mixing-limited rather than kinetically limited. This assumption allows simplification of the modeling and is justified when the model is compared against experimental results. Three test cases are used to validate the performance of the scramjet propulsion model: 1) a reflected-shock-tunnel hydrogen-fueled scramjet experiment, 2) a continuous-flow hydrogen-fueled scramjet ground test, and 3) a segment of the HyShot II flight test. The results show that the model simulates scramjet propulsion with a reasonable degree of accuracy.**

## Nomenclature

| | | |
|---|---|---|
| $A$ | = | geometric area of the duct, m$^2$ |
| $a_{1–6}$ | = | series of constants |
| $c$ | = | speed of sound, m/s |
| $c_f$ | = | skin-friction coefficient |
| $c_h$ | = | Stanton number |
| $c_p$ | = | specific heat, kJ/kgK |
| $D$ | = | chemical species |
| $\mathcal{D}$ | = | hydraulic diameter, m |
| $d$ | = | number of moles of species $D$ |
| $d$ | = | constant |
| $d_f$ | = | diameter of fuel injectors, m |
| FAS | = | stoichiometric fuel/air ratio |
| $f_c$ | = | fuel-mixture fraction along a centerline |
| $\bar{h}$ | = | mean specific enthalpy of a mixture, kJ/kg |
| $h_i$ | = | specific enthalpy of the ith species, kJ/kg |
| $K_p$ | = | equilibrium constant |
| $K^*$ | = | proportionality constant |
| $k$ | = | constant |
| $L$ | = | length, m |
| $M$ | = | Mach number |
| $Mc$ | = | convective Mach number |
| MW | = | molecular weight, kg/kmol |
| $\dot{m}$ | = | mass flow rate, kg/s |
| $N$ | = | number of moles |
| $Pr$ | = | Prandtl number |
| $Pr^*$ | = | modified Prandtl number |
| $P_w$ | = | perimeter of duct cross section, m |
| $p$ | = | pressure, Pa |
| $\mathcal{R}$ | = | universal gas constant, kJ/kgK |
| $Re$ | = | Reynolds number |
| $T$ | = | temperature, K |
| $U$ | = | velocity, m/s |
| $x$ | = | location along duct, m |
| $Y$ | = | mass fraction |
| $\alpha$ | = | variable |
| $\gamma$ | = | ratio of specific heats |
| $\delta$ | = | compressible turbulent mixing layer, m |
| $\delta_i$ | = | incompressible turbulent mixing layer, m |
| $\eta_m$ | = | mixing efficiency |
| $\theta$ | = | momentum thickness, m |
| $\kappa$ | = | constant |
| $\rho$ | = | density, kg/m$^3$ |
| $\phi$ | = | equivalence ratio |
| $\omega$ | = | ordinary-differential-equation solution |

*Subscripts*

| | | |
|---|---|---|
| $a$ | = | air |
| aw | = | adiabatic wall |
| $f$ | = | fuel |
| $fo$ | = | fuel at the injectors |
| $i$ | = | species |
| inj | = | injection conditions |
| mix | = | mixing conditions |
| mix, $i$ | = | incompressible mixing conditions |
| $w$ | = | wall |

## I. Introduction

THE development of supersonic combustion ramjet (scramjet) propulsion systems is accelerating, with recent flight-test successes demonstrating their viability [1,2]. This activity has renewed interest in predicting the performance of complete hypersonic vehicles using scramjet combustors, such as single-stage-to-orbit launch systems, long-range cruise vehicles, and missiles. The accurate prediction of vehicle performance early in the design process is vital if conceptual vehicles are to be successfully developed into complete systems in a timely manner. In addition, hypersonic vehicle performance calculators are useful for system analysis studies. To facilitate these activities, accurate and computationally efficient models of all aspects of the vehicle are required.

Quasi-one-dimensional modeling has been used in previous design and performance studies [3,4]. These models use a series of ordinary differential equations (ODEs) to model the flowfield and incorporate chemical kinetics as part of their thermodynamic description of the flow. Results from these studies show that scramjet performance is extremely sensitive to small changes in design, thermodynamic, and mixing parameters. It has been concluded from these studies that it is much better to design a scramjet to operate

Presented as Paper 4314 at the 18th AIAA Computational Fluid Dynamics Conference, Miami, FL; received 9 February 2009; accepted for publication 23 July 2009. 

*Research Fellow, School of Mechanical Engineering.
†Senior Lecturer, School of Mechanical Engineering. Senior Member AIAA.

using mixing-controlled combustion that is ignited via external or well-controlled means, rather than relying upon kinetically controlled ignition.

The aim of the present work is to develop a quasi-one-dimensional solver specifically designed to simulate the performance of scramjet combustors. The model uses a unique formulation of the gas dynamic equations incorporating an equation of state with equilibrium chemistry. Wall skin friction and heat transfer are also considered. It is assumed that supersonic combustion is mixing-controlled. This assumption is based on the calculated induction time for all cases being between 1 and 3 orders of magnitude quicker than the jet flow. In practice, this can be achieved by either a hot combustor inlet temperature (hence, negligible ignition delay) or by incorporating an igniter system into the scramjet, which effectively eliminates the ignition delay. It is shown that this assumption is valid, along with the assumption of equilibrium or simplified chemistry. Attention has been placed upon modeling the major processes associated with mixing and heat release, rather than the computationally expensive kinetics process.

## II. Quasi-One-Dimensional Flow Solver

The governing equations for the engine are formulated using a strategy similar to that in [3]. However, the current model assumes equilibrium chemistry or a "mixed-is-burned" combustion model that is mixing-limited rather than kinetically limited. This requires the problem to be treated as an open thermodynamic system, resulting in a new system of equations.

The governing equations are based on the following assumptions:

1) Quasi-one-dimensional flow (therefore, all flow variables) and the geometric area of the duct are functions of the axial distance $x$ along the duct.

2) The flow is steady state.

3) The flow behaves as an ideal gas.

### A. Conservation of Mass

Following [3], the conservation of mass in a steady-state flow is governed by the continuity equation:

$$\dot{m} = \rho U A \tag{1}$$

which can be expressed in a differential form as

$$\frac{1}{\dot{m}}\frac{\mathrm{d}\dot{m}}{\mathrm{d}x} = \frac{1}{\rho}\frac{\mathrm{d}\rho}{\mathrm{d}x} + \frac{1}{U}\frac{\mathrm{d}U}{\mathrm{d}x} + \frac{1}{A}\frac{\mathrm{d}A}{\mathrm{d}x} \tag{2}$$

What is important to appreciate from Eq. (2) is that changes in fuel injection and duct area can be incorporated using a mass injection rate $\mathrm{d}\dot{m}/\mathrm{d}x$ and an area profile $\mathrm{d}A/\mathrm{d}x$.

### B. Conservation of Momentum

The conservation of momentum is based on the quasi-one-dimensional formulation of [4]

$$\frac{1}{p}\frac{\mathrm{d}p}{\mathrm{d}x} + \frac{\gamma M^2}{2U^2}\frac{\mathrm{d}U^2}{\mathrm{d}x} + \frac{2\gamma M^2 c_f}{\mathcal{D}} + \frac{\gamma M^2}{\dot{m}}\frac{\mathrm{d}\dot{m}}{\mathrm{d}x} = 0 \tag{3}$$

The friction coefficient $c_f$ is calculated using an analytical technique [5], based on the reference enthalpy method. The hydraulic diameter is calculated from

$$\mathcal{D} = \frac{4A}{P_w} \tag{4}$$

### C. Equation of State

The equation of state for an ideal gas is

$$p = \frac{\rho \mathcal{R} T}{\overline{\mathrm{MW}}} \tag{5}$$

The differential form will be used to derive the quasi-one-dimensional model:

$$\frac{1}{p}\frac{\mathrm{d}p}{\mathrm{d}x} = \frac{1}{\rho}\frac{\mathrm{d}\rho}{\mathrm{d}x} + \frac{1}{T}\frac{\mathrm{d}T}{\mathrm{d}x} - \frac{1}{\overline{\mathrm{MW}}}\frac{\mathrm{d}\overline{\mathrm{MW}}}{\mathrm{d}x} \tag{6}$$

The mean molecular weight $\overline{\mathrm{MW}}$ allows for changes in species due to combustion and high-temperature effects. The mean molecular weight is defined using [3]

$$\overline{\mathrm{MW}} = 1 \Big/ \sum_i \frac{Y_i}{\mathrm{MW}_i} \tag{7}$$

The differential form allows the calculation of the variation of mean molecular weight along the duct:

$$\frac{\mathrm{d}\overline{\mathrm{MW}}}{\mathrm{d}x} = -\overline{\mathrm{MW}}^2\left(\sum_i \frac{1}{\mathrm{MW}_i}\frac{\mathrm{d}Y_i}{\mathrm{d}x}\right) \tag{8}$$

The model assumes that $i$ chemical species are present in the flowfield. The rate of change of each species mass fraction is determined by the rate of change of local equivalence ratio that, in turn, is set by the fuel injection rate along the duct. The changes in local equivalence ratio and species mass fraction are controlled by

$$\frac{\mathrm{d}\phi}{\mathrm{d}x} = \frac{\mathrm{d}\dot{m}_f}{\mathrm{d}x}\left(\frac{1}{\dot{m}_{a(\mathrm{FAS})}}\right) \tag{9}$$

$$\frac{\mathrm{d}Y_i}{\mathrm{d}x} = \frac{\mathrm{d}Y_i}{\mathrm{d}\phi}\frac{\mathrm{d}\phi}{\mathrm{d}x} \tag{10}$$

The rate of change of mass fraction with equivalence ratio is determined from the combustion model presented in Sec. II.F.

### D. Conservation of Energy

The differential form of the conservation of energy is derived using the formulation given by [6] and the control volume analysis of [3]. A modified version has been derived here to describe the energy flow in the scramjet combustor. This includes energy transported into the combustor by the fuel, energy liberated by combustion, and energy lost through heat transfer through the walls. This modified version is written as

$$\frac{\mathrm{d}h}{\mathrm{d}x} = \frac{h_f}{\dot{m}}\frac{\mathrm{d}\dot{m}_f}{\mathrm{d}x} - \frac{2c_f\bar{c}_p(T_{\mathrm{aw}} - T_w)}{Pr^{2/3}\mathcal{D}A} - \frac{h_0}{\dot{m}}\frac{\mathrm{d}\dot{m}_f}{\mathrm{d}x} - U\frac{\mathrm{d}U}{\mathrm{d}x} \tag{11}$$

Equation (11) has been derived using the Reynolds analogy that relates the skin-friction coefficient $c_f$ to the Stanton number $c_h$:

$$c_h = \frac{c_f}{2Pr^{2/3}} \tag{12}$$

The adiabatic wall temperature $T_{aw}$ for turbulent boundary layers is given by [5] as

$$T_{\mathrm{aw}} = T[1 + (Pr^*)^{1/3}\tfrac{1}{2}M^2(\gamma - 1)] \tag{13}$$

In all cases it has been assumed that

$$Pr = Pr^* = 0.71 \tag{14}$$

### E. Flowfield Enthalpy

It is assumed that the composition of the flowfield is set to be the product side of the single-step combustion reaction mechanism:

$$\phi(\mathrm{fuel}) + \mathrm{air} \rightarrow \mathrm{products} \tag{15}$$

The fuel can be either hydrogen or a hydrocarbon fuel (ethylene, jet A, etc.) and the equivalence ratio $\phi$ determines the composition of the products. The products are either set to the major species ($O_2$, $N_2$, $H_2O$, and $CO_2$) or are in thermodynamic chemical equilibrium. For the current paper, only hydrogen fuel is considered.

In either case, the flowfield thermodynamic chemical equilibrium will be a function of the pressure $p$, equivalence ratio $\phi$, and the temperature $T$:

$$h = h(p, \phi, T) \tag{16}$$

The differential form of the flowfield enthalpy can then be written as

$$\frac{\mathrm{d}h}{\mathrm{d}x} = \left(\frac{\partial h}{\partial p}\right)\frac{\mathrm{d}p}{\mathrm{d}x} + \left(\frac{\partial h}{\partial \phi}\right)\frac{\mathrm{d}\phi}{\mathrm{d}x} + \left(\frac{\partial h}{\partial T}\right)\frac{\mathrm{d}T}{\mathrm{d}x} \tag{17}$$

Combining Eqs. (11) and (17) produces an expression for the temperature gradient:

$$\frac{\mathrm{d}T}{\mathrm{d}x} = \left(\frac{\partial h}{\partial T}\right)^{-1}\left\{\left[\frac{h_f}{\dot{m}}\frac{\mathrm{d}\dot{m}_f}{\mathrm{d}x} - \frac{2c_f\bar{c}_p(T_{\mathrm{aw}} - T_w)}{Pr^{2/3}\mathcal{D}A} - \frac{h_0}{\dot{m}}\frac{\mathrm{d}\dot{m}_f}{\mathrm{d}x} - U\frac{\mathrm{d}U}{\mathrm{d}x}\right] - \left(\frac{\partial h}{\partial p}\right)\frac{\mathrm{d}p}{\mathrm{d}x} - \left(\frac{\partial h}{\partial \phi}\right)\frac{\mathrm{d}\phi}{\mathrm{d}x}\right\} \tag{18}$$

The partial derivatives of enthalpy [Eq. (16)] are determined numerically using the combustion model detailed next.

### F. Combustion Model

The flowfield enthalpy is determined from [7] as

$$\bar{h} = \sum_i h_i Y_i \tag{19}$$

The individual enthalpies are calculated from the NASA polynomials [8]:

$$h_i = \left(\frac{RT}{\mathrm{MW}_i}\right)\left(a_{1,i} + \frac{a_{2,i}}{2}T + \frac{a_{3,i}}{3}T^2 + \frac{a_{4,i}}{4}T^3 + \frac{a_{5,i}}{5}T^4 + \frac{a_{6,i}}{T}\right) \tag{20}$$

where $a_{1\text{–}6}$ are a series of constants for species $i$, based on two different temperature ranges. The individual species specific heats are also calculated from the NASA polynomials [8] as

$$c_{p,i} = \left(\frac{\mathcal{R}}{\mathrm{MW}_i}\right)(a_{1,i} + a_{2,i}T + a_{3,i}T^2 + a_{4,i}T^3 + a_{5,i}T^4) \tag{21}$$

Determination of the species mass fraction can be achieved using either a simplified combustion model or a model that assumes thermodynamic chemical equilibrium.

In the simplified model, the products are limited to the major species ($O_2$, $N_2$, and $H_2O$) and the mass fractions are set according to a global chemical reaction mechanism [Eq. (15)] that accounts for the atom balance between reactants and products.

### G. Complete Equation Set

Combining Eqs. (2), (3), (6), and (17) gives the differential equation for velocity in the duct as

$$\frac{\mathrm{d}U}{\mathrm{d}x} = \frac{1}{\alpha}\left\{-\frac{1}{A}\frac{\mathrm{d}A}{\mathrm{d}x} + \frac{1}{\dot{m}}\frac{\mathrm{d}\dot{m}}{\mathrm{d}x}\left[1 + \gamma M^2 A_0 + \frac{1}{T}\left(\frac{\partial \bar{h}}{\partial T}\right)^{-1}(\bar{h}_f - \bar{h}_0)\right] - \frac{1}{\overline{\mathrm{MW}}}\frac{\mathrm{d}\overline{\mathrm{MW}}}{\mathrm{d}x} + \frac{2c_f}{\mathcal{D}}\left[\gamma M^2 A_0 - \frac{\bar{c}_p(T_{\mathrm{aw}} - T_w)}{Pr^{2/3}}\frac{1}{T}\left(\frac{\partial \bar{h}}{\partial T}\right)^{-1}\right] - \frac{1}{T}\left(\frac{\partial \bar{h}}{\partial \phi}\right)\frac{d\phi}{dx}\left(\frac{\partial \bar{h}}{\partial T}\right)^{-1}\right\} \tag{22}$$

$$A_0 = 1 + \frac{p}{T}\left(\frac{\partial \bar{h}}{\partial T}\right)^{-1}\left(\frac{\partial \bar{h}}{\partial p}\right) \tag{23}$$

$$\alpha = \frac{1}{U}\left[1 - \gamma M^2 A_0 + \frac{U^2}{T}\left(\frac{\partial \bar{h}}{\partial T}\right)^{-1}\right] \tag{24}$$

The equations derived previously now represent a set of stiff ODEs that can be solved using an ODE solver in a space-marching technique. Using the equation of state with conservation of mass and energy allows closure of the equation set:

$$\frac{\mathrm{d}\rho}{\mathrm{d}x} = \rho\left[\frac{1}{\dot{m}}\frac{\mathrm{d}\dot{m}}{\mathrm{d}x} - \frac{1}{U}\frac{\mathrm{d}U}{\mathrm{d}x} - \frac{1}{A}\frac{\mathrm{d}A}{\mathrm{d}x}\right] \tag{25}$$

$$\frac{\mathrm{d}p}{\mathrm{d}x} = -\gamma\rho M^2\left[\frac{1}{U}\frac{\mathrm{d}U}{\mathrm{d}x} + \frac{1}{2}\left(\frac{4c_f}{\mathcal{D}}\right) + \frac{1}{\dot{m}}\frac{\mathrm{d}\dot{m}}{\mathrm{d}x}\right] \tag{26}$$

The ODEs are solved using a fourth-order Runge–Kutta method. The computational time to solve for any of the cases investigated with 1000 time steps is less than 7 s using a MacBook with 2 GHz Intel Core 2 Duo processor and 1 GB 667 MHz memory.

### H. Supersonic Mixing Model

The key to accurate combustor performance simulation is determining the correct release of energy along the duct. In the current model, this is performed by deriving a supersonic mixing model.

Typically, mixing of fuel and air is calculated by solving the Navier–Stokes equations in conjunction with a turbulence model. To keep the computational overheads low, the problem is simplified using the concept of mixing efficiency, which is defined as the ratio of fuel that is available for combustion to the amount that was injected. A relation specifically for mixing efficiency in scramjet combustors is derived using results from the literature.

It is assumed that the fuel available for reaction can be determined using a mixing efficiency

$$\dot{m}_f = \eta_m \dot{m}_{f0} \tag{27}$$

where $\dot{m}_f$ is the mass flow rate of fuel available for reaction, $\eta_m$ is the mixing efficiency, and $\dot{m}_{f0}$ is the mass flow rate of fuel through the injectors. The mixing efficiency changes in value from zero at the injector exit until it reaches unity at a defined mixing length $L_{\mathrm{mix}}$, where all the available fuel is mixed with the combustor air and is ready for combustion. Reference [9], in their work on scaling supersonic flames, derived fuel-mixture-fraction profiles along the centerlines of incompressible jets:

$$f_{\mathrm{cl}} = \kappa\left[\left(\frac{\rho_f U_f}{\rho_a U_a}\right)\right]\left(\frac{x}{d_f}\right)^{-2} \tag{28}$$

Assuming $x = L_{\mathrm{mix},i}$ (the incompressible mixing length), rearranging Eq. (28) shows that the incompressible mixing length is

$$\frac{L_{\mathrm{mix},i}}{d_f} \propto \left[\frac{\rho_f U_f}{\rho_a U_a}\right]^{1/2} \tag{29}$$

Reference [10] shows that the rate of growth of a compressible turbulent mixing layer $\mathrm{d}\delta/\mathrm{d}x$ is related to the convective Mach number $M_c$ and incompressible growth rate $\mathrm{d}\delta_i/\mathrm{d}x$ by a function dependent on $M_c$. It is assumed that mixing length is inversely proportional to the mixing-layer growth rate:

$$L_{\mathrm{mix}} \propto \left(\frac{\mathrm{d}\delta}{\mathrm{d}x}\right)^{-1} \tag{30}$$

Hence, compressible and incompressible mixing lengths are related by

$$L_{\mathrm{mix}} = L_{\mathrm{mix},i} \times \frac{1}{f(M_c)} \tag{31}$$

given

$$f(M_c) = 0.25 + 0.75e^{-3M_c^2} \qquad M_c = \frac{U_f - U_a}{a_f + a_a} \tag{32}$$

By using the proportionality constant $K^*$, the compressible mixing length can be written

$$\left(\frac{L_{\mathrm{mix}}}{d_f}\right) = \frac{K^*}{f(M_c)}\left[\frac{\rho_f U_f}{\rho_a U_a}\right]^{1/2} \tag{33}$$

The constant $K^*$ is found by using the multidimensional computational fluid dynamics results of [11]. In their work, mixing efficiency was calculated along a hydrogen-fueled strut-injected scramjet duct and compared with experimental measurements. These results show that mixing efficiency is reasonably independent of injector nozzle exit dimensions. Using the results from this study, the value of the constant was found to be $K^* = 390$ and mixing efficiency was found to have the form

$$\eta_m = a(1 - e^{(-(k\bar{x})^d)}) \quad a = 1.06492 \quad k = 3.69639 \quad d = 0.80586 \tag{34}$$

where

$$\bar{x} = \frac{x - L_{\text{inj}}}{L_{\text{mix}}} \tag{35}$$

Hence, an efficient method is available to calculate the mixing efficiency and amount of fuel available for reaction. In all test cases presented in this paper, Eq. (34) is differentiated and used in a differential form of Eq. (27) to calculate mixing efficiency. The mixing length is either calculated using Eq. (33) for strut-injected engines or is specified by the user for other types of fuel injection. It should be noted that there are no known published values of $K^*$ for any fuel injection system other than strut injection systems. This results from a lack of experimental data. For fuel injection types other than strut injections, the value of $L_{\text{mix}}$ is estimated. When experimental data are made available to determine $K^*$ for other injection systems, the current model can be reassessed. Nonetheless, as a measure of the sensitivity of $K^*$ for strut injection, it has been determined that a $\pm 10\%$ variation in $K^*$ results in a variation of less than $\pm 2.9\%$ to the calculated peak pressure for test case 1, shown next.

## III. Comparison with Experimental Data

### A. Test Case 1: Reflected-Shock-Tunnel Experiment

Reference [12] conducted experiments in the T4 free-piston reflected-shock tunnel at The University of Queensland. As this type of facility has a steady test period of approximately 1 ms, reflected-shock tunnels are described as pulse facilities to describe the transient nature of the test flow. The scramjet test simulated here used a diverging duct in which both the top and bottom plates of the scramjet were set to 1.72 deg. Supersonic air at Mach 2.47, a temperature of 1025 K, and a static pressure of 59 kPa was generated at the entrance to the combustion chamber, which represents a flight Mach number of approximately 7. Hydrogen fuel was injected at sonic conditions using a central strut to achieve an overall equivalence ratio of 0.38. Figure 1 is a schematic diagram of the modeled component of the experimental arrangement used by [12].

Figure 2 compares the experimental scramjet combustor measurements of [12] with numerical data generated using the quasi-one-dimensional model. The model does not resolve the pressure fluctuations associated with the weak two-dimensional shock waves generated by the central strut injector (duct length is 0 m), and it does not accurately predict the peak pressure. However, it does successfully reproduce the mean pressure rise along the duct. By simulating the mean pressure distribution along the combustor correctly along with wall skin-friction losses, the quasi-one-dimensional model is capable of calculating the thrust and specific impulse of a scramjet combustor. As the model is also computationally efficient, it can be directly incorporated into design optimization, performance, and trajectory simulations and called repeatedly during the solution time.

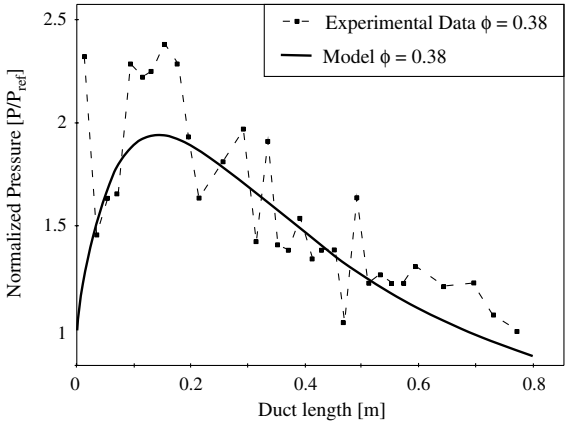


**Fig. 2 Pressure comparison of ground-test data from [12] with current results.**

### B. Test Case 2: University of Virginia Supersonic Combustion Experiments

Reference [13] conducted experiments in the University of Virginia supersonic combustion facility. The geometry of their facility consists of a constant area rectangular duct, followed by a divergence of the duct ceiling by an angle of 2.9 deg (Fig. 3). A ramp injector was used for hydrogen fuel injection into the hot supersonic test gas. Supersonic air was provided with a Mach number of 2.1, static temperature of 670 K, and a static pressure of 39 kPa, which represents a flight Mach number of approximately 5. Ignition was performed using a hydrogen–oxygen detonation-driven ignition system, and combustion was self-sustaining after ignition. Two cases are investigated in this study. The first is a case in which no fuel was injected, and the second is a case in which hydrogen fuel was injected sonically from the ramp injector so that the overall equivalence ratio was $\phi = 0.32$.

Figure 4 compares both the fuel-off and the fuel-on experimental results of [13] with simulation results obtained from the quasi-one-dimensional model. The fuel-off experimental data show pressure fluctuations along the duct due to weak shocks generated by the ramp injector. Although the quasi-one-dimensional model does not capture these, it does reproduce the mean pressure distribution along the duct. The large pressure rise at the downstream end of the results is due to an exhaust shock that compresses the test flow to atmospheric conditions. This was not modeled using the quasi-one-dimensional solver.

Figure 4 also compares supersonic combustion data with simulation results for an equivalence ratio of $\phi = 0.32$. Again, the model adequately resolves the mean pressure rise; however, to obtain this

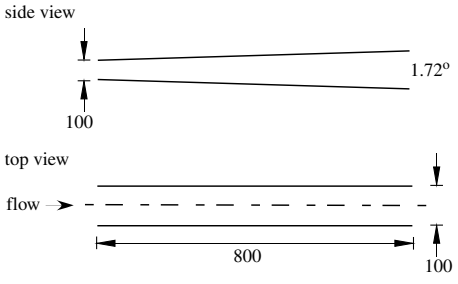


**Fig. 1 Schematic diagram of the experimental arrangement used by [12].**

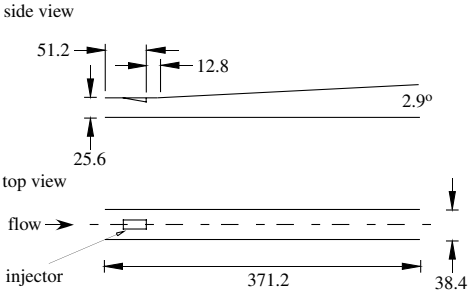


**Fig. 3 Schematic diagram of the University of Virginia supersonic combustion facility from [13]; units are in millimeters.**

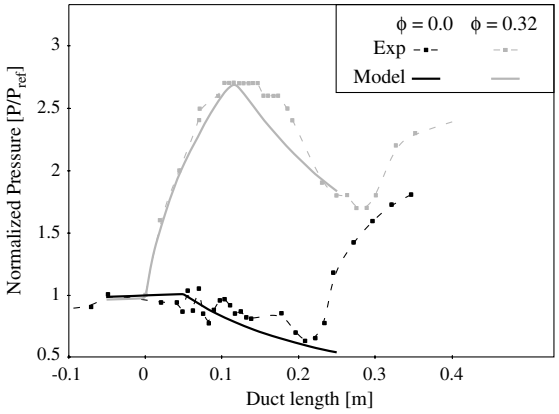


**Fig. 4 Pressure comparison of ground-test data from [13] with current results ($P_{\text{ref}} = 40$ kPa).**

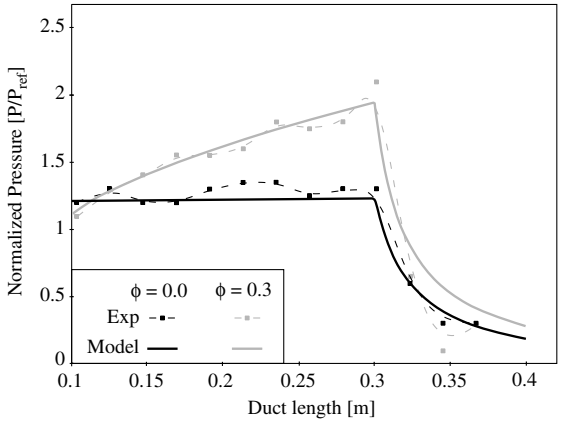


**Fig. 6 Pressure comparison of flight data from [1] with current results ($P_{\text{ref}}$ is the flight-test pitot pressure).**

result, the mixing-length was estimated to be longer than the engine ($L_{mix} = 4.15$ m), resulting in a combustion efficiency of 90.3%. For values of $L_{\text{mix}} < 0.415$ m, the choking limit is reached. As discussed in Sec. II.H, the mixing length for a non-strut-injection system cannot be determined using Eq. (33), as no empirically determined value of $K^*$ is available.

It is interesting to observe that the experimental results for the fuel-on case show a plateau in pressure between 0.1 and 0.18 m, whereas the model pressure peaks at 0.1 m before monotonically decreasing. This may be explained by the fact that the mixing model used in the numerical model was derived from nonreacting, cold, supersonic mixing data for a central strut, and the Mach number in the duct approaches unity. The ramp injector achieves rapid mixing using a pair of counter-rotating vortices that are not present during central strut injection. The mixing-length model used here is modified to incorporate this effect by approximating its value, but this modification is not adequate to perfectly resolve this pressure plateau. Nevertheless, the model still achieves a remarkable reproduction of the scramjet flowfield, suitable for use in performance studies. It should be noted that [13] also presents a prediction using the multidimensional GASPex version 3.2 code. Their predictions (not shown in the current report) show a similar peak instead of a plateau.

### C. Test Case 3: HyShot II Flight Tests

Flight tests of the HyShot II program [1] are also used for validation study. The HyShot II combustor is a 300-mm-long, 9.8 × 75 mm duct followed by a 147-mm-long, 12 deg divergence of the duct ceiling (Fig. 5). Fuel injection into the HyShot combustor was achieved via circular fuel injection ports (4 × 2 mm in diameter) in the floor of the combustor, 58 mm from the entrance. Two flight conditions are simulated in this study: both are at an altitude of 33 km and at a Mach number of approximately 7.7.

The first flight-test experiment was obtained with no fuel injection and while the vehicle was traveling at an angle of attack of 5.26 deg at Mach 7.75. The hypersonic inlet supplied the combustor with supersonic air at a Mach number of 2.0, a temperature of 1571 K, and a pressure of 65.9 kPa. The second flight-test experimental result was obtained with fuel injection and with the vehicle at an angle of attack of 4.26 deg and a Mach number of 7.74. The combustor inlet was supplied with supersonic air at a Mach number of 2.0, a temperature of 1528 K, and a pressure of 73.76 kPa. The nominal equivalence ratio was 0.3 for this experiment. Figure 6 compares both fuel-off and fuel-on experimental results with numerical data obtained from the quasi-one-dimensional solver. The fuel-off experimental results are matched well by the solver, indicating that the model is correctly modeling gas dynamics and viscous losses acting internally within the engine.

The fuel-on experimental results show that the pressure rise is delayed beyond what would be considered normal in a hot, turbulent, supersonic combustor. It is postulated here that the hydrogen fuel is initially injected into a laminar boundary layer. This therefore limits mixing to that achievable by molecular diffusion, which is very low. It is not until the mixing rate is suddenly increased at a position of approximately 100 mm from the combustor leading edge that significant pressure rise due to supersonic combustion can be measured. It is unclear what exactly causes this, but it is reasonable to expect that turbulent transition of the boundary layer or shock-induced mixing enhancement from the reflected injection shock from the duct cowl will rapidly increase the mixing rate. It is likely that both of these phenomena are coupled within the combustor.

For the HyShot test case, it was assumed that the initial molecular diffusion phase of supersonic mixing was negligible. Fuel injection was therefore initiated at 100 mm from the combustor entrance. Figure 6 compares the simulation results against the fuel-on experimental data and shows a reasonable comparison. To achieve this result, a mixing length of $L_{\text{mix}} = 0.9$ m was required, which resulted in incomplete combustion at the combustor exit, with a predicted combustion efficiency of 78.3%. As discussed in Sec. III.B, the mixing length for the non-strut-injection systems (such as the HyShot configuration) cannot be determined using Eq. (33), as no empirically determined value of $K^*$ is available to assess the suitability of the current selection of the mixing length.

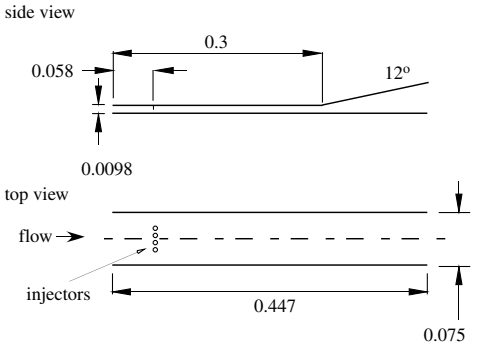


**Fig. 5 Schematic diagram of the experimental HyShot II combustion duct from [1]; units are in millimeters.**

## IV. Conclusions

A quasi-one-dimensional model has been developed and used to describe hydrogen-fueled scramjet combustor reacting flows in a high-enthalpy-pulse facility experiment, a continuous-flow supersonic combustion facility ground test, and the HyShot II flight test. In each test case, the model is capable of simulating the mean pressure distribution along the combustor, therefore making it suitable to predict the performance of conceptual scramjet vehicles. The model is also useful for the analysis of ground-test and flight data, increasing understanding concerning mixing and combustion phenomena within the scramjet combustor.

## Acknowledgments

This work was supported by the Defence Science and Technology Organisation, Weapons Systems Division.

## References

[1] Smart, M. K., Hass, N. E., and Paull, A., "Flight Data Analysis of the HyShot 2 Scramjet Flight Experiment," *AIAA Journal*, Vol. 44, No. 10, 2006, pp. 2375–2366. doi:10.2514/1.20661

[2] Moses, P. L., Rausch, V. L., Nguyen, L. T., and Hill, J. R., "NASA Hypersonic Flight Demonstrators Overview, Status and Future Plans," *Acta Astronautica*, Vol. 55, Nos. 3–9, 2004, pp. 619–630. doi:10.1016/j.actaastro.2004.05.045

[3] OBrien, T., Starkey, R., and Lewis, M., "Quasi-One-Dimensional High-Speed Engine Model with Finite Rate Chemistry," *Journal of Propulsion and Power*, Vol. 17, No. 6, 2001, pp. 1366–1374. doi:10.2514/2.5889

[4] Starkey, R. P., and Lewis, M. J., "Sensitivity of Hydrocarbon Combustion Modeling for Hypersonic Missile Design," *Journal of Propulsion and Power*, Vol. 19, No. 1, 2003, pp. 89–97. doi:10.2514/2.6084

[5] Anderson, J. D., *Hypersonic and High Temperature Gas Dynamics*, AIAA, Reston, VA, 2000.

[6] Turns, S. R., *An Introduction to Combustion*, McGraw–Hill, New York, 1996.

[7] Kee, R. J., Rupley, F. M., and Miller, J. A., "Chemkin-II: A Fortran Chemical Kinetics Package for the Analysis of Gas-Phase Chemical Kinetics," Sandia National Labs., Rept. SAND89-8009, Albuquerque, NM, 1989.

[8] Gordon, S., and McBride, B. J., "Computer Program for Calculation of Complex Chemical Equilibrium Compositions, Rocket Performance, Incident and Reflected Shocks, and Chapman-Jouguet Detonations," NASA SP-273, 1976.

[9] Driscoll, J. F., Huh, H., Yoon, Y., and Donbar, J., "Measured Lengths of Supersonic Hydrogen-Air Jet Flames—Compared to Subsonic Flame Lengths—and Analysis," *Combustion and Flame*, Vol. 107, Nos. 1–2, 1996, pp. 176–186. doi:10.1016/0010-2180(96)00048-X

[10] Papamoschou, D., and Roshko, A., "The Compressible Turbulent Shear Layer: An Experimental Study," *Journal of Fluid Mechanics*, Vol. 197, No. -1, 1988, pp. 453–477. doi:10.1017/S0022112088003325

[11] Gerlinger, P., and Brüggemann, D., "Numerical Investigation of Hydrogen Strut Injections into Supersonic Airflows," *Journal of Propulsion and Power*, Vol. 16, No. 1, 2000, pp. 22–28. doi:10.2514/2.5559

[12] Boyce, R. R., Paull, A., Stalker, R. J., Wendt, M., Chinzei, N., and Miyajima, H., "Comparison of Supersonic Combustion Between Impulse and Vitiation-Heated Facilities," *Journal of Propulsion and Power*, Vol. 16, No. 4, 2000, pp. 709–717. doi:10.2514/2.5631

[13] Goyne, C. P., McDaniel, J. C., Quagliaroli, T. C., Krauss, R. H., and Day, S. W., "Dual-Mode Combustion of Hydrogen in a Mach 5, Continuous-Flow Facility," *Journal of Propulsion and Power*, Vol. 17, No. 6, 2001, pp. 1313–1318. doi:10.2514/2.5880

R. Bowersox
*Associate Editor*